Simultaneous detection of pH value and key-metabolite concentrations for wound monitoring applications

D. A. Jankowska[a,†], M. B. Bannwarth[b,†], C. Schulenburg[a], G. Faccio[a], K. Maniura-Weber[a], R. M. Rossi[b], L. Scherer[b], M. Richter[a,*] & L. F. Boesel[b,*]

[a] Empa - Swiss Federal Laboratories for Materials Science and Technology, Laboratory for Biointerfaces, Lerchenfeldstrasse 5, 9014 St. Gallen (CH)

[b] Empa - Swiss Federal Laboratories for Materials Science and Technology, Laboratory for Protection and Physiology, Lerchenfeldstrasse 5, 9014 St. Gallen (CH)

† These authors contributed equally to this work (D.A.J., M.B.B.)

* Corresponding author: Dr. Michael Richter. Current address: Fraunhofer Institute for Interfacial Engineering and Biotechnology IGB, Bio-, Electro- and Chemocatalysis BioCat, Straubing Branch, Schulgasse 11a, 94315 Straubing (DE), Tel: +49 9421 187 353, Email: michael.richter@igb.fraunhofer.de

* Corresponding author: Dr. Luciano F. Boesel, Protection and Physiology, Empa - Swiss Federal Laboratories for Materials Science and Technology, Lerchenfeldstrasse 5, 9014 St. Gallen (CH), Tel: +41 58 765 7393, Email: luciano.boesel@empa.ch

Abstract

Aging population and longer life expectancy are the main reasons for an increasing number of patients with wound problems. Although the interest in wound care increases continuously, wound management still remains a challenge mainly due to the higher occurrence of chronic wounds, which require intensive care and constant monitoring. Here, we demonstrate a fluorescent sensing system to monitor the wound status and to distinguish between an autonomously healing and a chronic wound at an early stage. The system allows monitoring two of the most relevant fluctuating wound parameters during the healing process which are pH and glucose concentration. A fluorescent pH indicator dye, carboxynaphthofluorescein, and a metabolite-sensing enzymatic system, based on glucose oxidase and horseradish peroxidase, were immobilized on a biocompatible polysaccharide matrix to develop a functional hydrogel coating for wound monitoring. The changes in metabolite and enzyme concentration in artificial wound extract were converted into a fluorescent signal.

Keywords: biosensor, wound monitoring, pH sensing, glucose sensing, metabolites, functional hydrogels

Introduction

Chronic wounds are one of the most common health problems of elderly people (Sen et al. 2009). Current wound management includes the frequent change of wound dressings and the assessment of the color or odor of the wound exudate (Grey et al. 2006; Mehmood et al. 2014). Besides giving only subjective information on the wound status, the frequent change of the dressing may result in skin irritation, in damage of the newly grown tissue and in an increased risk of infection. As a consequence, the wound healing process may be delayed. Normally, hospitalization is required for a permanent monitoring and treatment of a wound, which leads to longer treatment duration for the patient and enormous costs (Sen et al. 2009).

To overcome unnecessary removal of the dressing, novel non-invasive monitoring systems have to be developed. A chronic wound offers multiple opportunities for monitoring since it undergoes various stages at a molecular level before reaching complete recovery (Velnar et al. 2009). The different stages of the healing process are accompanied by specific and dynamic changes in the composition of the wound exudate in terms of pH and metabolites which can serve as biomarkers reflecting the current wound status (Dargaville et al. 2013; Eming et al. 2010; Trengove et al. 1996; Velnar et al. 2009). pH is one of the most important wound parameters and depends on time course and wound-stage. During normal healing, pH increases during granulation and decreases afterwards to reach a value of 4-6. During impaired healing the pH oscillates between pH 7-8 (Dargaville et al. 2013; Schneider et al. 2007) and this rather large difference in pH between two types of wounds can be sensitively detected. Another wound marker is glucose concentration which was found to correlate with the healing status. The glucose concentration is higher for acute wounds and its monitoring may be an important indicator for healing especially for diabetic patients (Krismastuti et al. 2014; Trengove et al. 1996).

Different types of sensors have been developed to monitor the changes occurring in the wound. Current research is trending towards miniaturized wearable devices for continuous measurement. One example is a moisture sensor based on electrical impedance measurement. The sensor sits directly on the wound and the readouts are displayed on an

external device connected by a cable. This instrument, named WoundSenseTM, has been commercialized (McColl et al. 2007; Milne et al. 2015). A more advanced but not yet available sensor was presented by Mehmood et al. (2015). Their telemetric sensing system monitors three parameters of the wound – temperature, moisture and pressure – and transmits the data wirelessly to a portable unit with a display. A few miniaturized devices were also developed for the monitoring of pH (Phair et al. 2011) and of bacterial infection (Hajnsek et al. 2015). These kinds of sensors are effective, but are meant for external use and require interference with the wound in order to collect the wound liquid. Only a few sensors have been designed to give a visible signal directly on the wound pad without the need to use electronic parts or devices for readout. Those dressings release fluorescent dyes upon contact with bacterial virulence factors like toxins (Thet et al. 2016) or enzymes (Ebrahimi and Schonherr 2014). The signals can be detected under an UV lamp with the naked eye. In general, such responsive dressings are of a simple structure, built of a hydrogel such as agarose or chitosan with embedded sensors molecules. The matrices are known to be biocompatible in the wound context and available on the market as standard moisture-spending dressings. Since no electronics are needed to read the signal, those sensors are easier to manufacture and should become widely available. However, the signal obtained from the described wound pads cannot be quantified.

We have recently developed chemical and bio-sensors based on fluorescence changes for different applications. pH sensors were constructed by incorporating a FRET-forming dye pair into xerogel matrices (Widmer et al. 2014; Widmer et al. 2015). Fluorescein, a pH sensitive dye, was used as donor or acceptor in the matrices. The system was reversible and could be used as coating for a range of substrates, including plates, optical fibers, and textiles (Widmer et al. 2014; Widmer et al. 2015). We further developed FRET-based systems to detect metabolites as glucose and maltose, or enzymes like neutrophil elastase with very high sensitivity (Faccio et al. 2016; Schulenburg et al. 2016). By encapsulating maltose or glucose sensitive proteins into silica particles, we were able to increase the stability of the protein biosensor towards chemical and thermal denaturation while preserving their activity and affinity (Faccio et al. 2016). Our FRET-based sensor designed to detect neutrophil elastase showed up to 500 higher specificity to the enzyme than other commercially available substrates for neutrophil elastase (Schulenburg et al. 2016). However, the

integration of these FRET-based systems into wound pads can be tricky. Hence, we proposed a simple system based on the immobilization of a single dye and enzymes in hydrogel matrices. This paper presents the concept and design of the smart wound pad as well as activity and stability studies of the enzymes in solution and within a polymeric matrix in buffer and in complex artificial wound extract. The system comprises the use of natural polymers matrix with a pH-sensitive dye and a metabolite indicating system (Figure 1). Hereby pH sensing is achieved by the highly pH-responding fluorescent dye, 5(6)-carboxynaphthofluorescein, which is especially sensitive in the pH-range 6 to 8 that occurs in chronic wounds. Metabolite sensing is accomplished by a coupled enzyme reaction in which the two enzymes glucose oxidase (GOx) and horseradish peroxidase (HRP) react sequentially, and GOx produces a substrate for HRP. Fluorescein serves as a second substrate of HRP. Upon the enzyme-catalyzed oxidation of the fluorescent probe, the product is leading to a quantitative fluorescence signal, allowing for highly sensitive wound marker detection. Our modular system is designed for easy adaptation to detect other key wound marker metabolites. Hence, simultaneous detection of pH and various metabolites may allow for comprehensive wound monitoring in parallel.

Materials and Methods

Enzymes and chemicals

The enzymes glucose oxidase and horseradish peroxidase type II and substrates 2,2'-Azino-bis(3-ethylbenzothiazoline-6-sulfonic acid) diammonium salt (ABTS), 2',7'-dichlorofluorescin-diacetate (H_2DCF-DA), 5(6)-carboxynaphthofluorescein (CNF), 4- dimethylaminopyridine (DMAP), sodium alginate, sodium periodate, ethyleneglycol, sodium chloride and N,N-dicyclohexylcarbodiimide (DCC) were purchased from Sigma Aldrich (Buchs, CH). Dimethylformamide (DMF; Sigma Aldrich, Buchs, CH) was dried over 4 Å molecular sieves before use. Ethanol was purchased from Fluka (Buchs, CH).

Solutions and media

All measurements were conducted in PBS buffer, Dulbecco's Modified Eagle's Medium (DMEM) (Sigma-Aldrich, Buchs, CH) solubilized in PBS buffer (pH 6.2), or artificial wound exudate (Campbell et. al (2003) with following modification: AWE = DMEM solubilized in PBS buffer (pH 6.2), including 10% (v/v) porcine serum (Gibco, Lucerne, CH)).

Determination of protein concentration

Glucose oxidase concentration was determined by absorbance spectroscopy (Nanodrop, Thermo Scientific, Reinach, CH) using the extinction coefficient of 267.2 mM^{-1} cm^{-1} at 280 nm, and for horseradish peroxidase concentration the extinction coefficient of 100 mM^{-1} cm^{-1} at 403 nm was used. The concentration of ABTS was determined using the extinction coefficient of 36800 M^{-1} cm^{-1} at 410 nm.

Horseradish peroxidase activity assay using ABTS as substrate

Kinetic measurements of horseradish peroxidase using ABTS and H_2O_2 as substrates were performed at 33°C on a 96-well plate in a plate reader (BioTek Synergy Mx) using a final enzyme concentrations of 0.1 to 2 nM in PBS pH 6.2, DMEM medium or artificial wound exudate. Initial rates were determined by monitoring the increase in signal at 410 nm. Initial velocities were plotted as a function of H_2O_2 or ABTS concentration, respectively, and the steady-state parameters k_{cat} and K_M were determined using the Michaelis-Menten equation ($v = \frac{V_{max}[S]}{K_M+[S]}$); with v: reaction rate, V_{max}: maximum rate, [S]: substrate concentration, K_M: Michaelis constant).

Activation of 2',7'-dichlorofluorescin, H_2DCF-DA

For H_2DCF-DA activation, H_2DCF-DA was dissolved in DMSO to yield a concentration of 11.5 mM. Activation was initiated by five-fold dilution in 0.01 M NaOH. The solution was stirred in the dark at room temperature (RT) for 30 min to form 2`7`dichlorodihydrofluorescein (H_2DCF). This solution was subsequently 20-fold diluted in the PBS appropriate buffer pH 6.2.

Horseradish peroxidase activity assay using H_2DCF as substrate

Kinetic measurements using H_2DCF as substrate were performed at room temperature on a fluorescence plate reader (Varian, Cary Eclipse) using final enzyme concentrations of 20 to 40 nM in PBS pH 6.2, or AWE. H_2DCF fluorescence was excited at 485 nm and initial rates determined by monitoring the increase in signal at 528 nm. Product formation was calculated using a calibration curve with fully oxidized 2`7`dichlorofluorescein (DCF). For this, H_2DCF was oxidized in the presence of 2 mM $KMnO_4$. Initial velocities were plotted versus

H_2O_2 or ABTS concentration, and the steady-state parameters k_{cat} and K_M were determined using the Michaelis-Menten equation (described above).

Enzyme-coupling to the polymer matrix

Sodium alginate was dissolved in water (2% w/v) and mixed with a solution of sodium periodate in water (4% w/v) to prepare oxidized alginate. The reaction was allowed to proceed overnight. The yellowish and viscous compound was then purified by sequential addition of ethyleneglycol, sodium chloride, and ethanol.

Next, 240 mg of oxidized alginate and 240 mg of sodium alginate (to promote a better gelation after enzyme coupling) were dissolved in 48 mL PBS buffer at pH 6.2 in the dark. The respective enzymes were added to yield final enzyme concentrations of 20 nM HRP and 0.1 nM GOx. The mixture was stirred overnight and $NaBH_4$ was added to reduce the imine-linkage between enzyme and oxidized alginate to the corresponding amine. After stirring for 2 h, 100 µL aliquots of the enzyme-alginate conjugate were added to a well plate and the gelation was initiated by the addition of 5 µL aqueous solution of 2% calcium chloride (w/v). The well plates were left at 4°C overnight for complete gelation before further investigation.

pH-dye coupling to the polymer matrix

100 mg of agarose, 5 mg of CNF and 0.5 mg of DMAP were dissolved in 5 mL of DMF and cooled down to 2°C on ice. Subsequently, 3 mg of DCC was added and the solution kept for 5 min at 2°C before removing the ice bath and stirring in the dark and at room temperature overnight. The modified agarose was precipitated through addition of acetone. Subsequently, it was separated and re-dissolved in water before precipitation in acetone for removal of the residual impurities. The brown solid was dried under vacuum overnight. The fluorescent properties of the CNF were determined at λ_{ex} = 600 nm and λ_{em} between 640-740 nm.

Determination of GOx activity in solution using the coupled enzyme assay with H_2DCF as substrate

For the coupled enzyme assay 0.1 mM H_2DCF, 0.1 nM GOx, 20 nM HRP and 0-200 mM glucose in a total volume of 100 µL or 200 µL were used. Initial rates were determined as described above, using the change in signal upon DCF formation at 528 nm.

Activity of immobilized HRP and GOx

Activity of immobilized HRP was determined at RT under saturating substrate concentrations (50 µM H_2O_2 and 0.1 mM H_2DCF). Activity of immobilized GOx was determined at RT under saturating H_2DCF concentration for HRP (0.1 mM H_2DCF). To initiate the reaction, 100 µL of substrate mixture (in PBS pH 6.2) containing 0.1 mM H_2DCF with 50 µM H_2O_2 (for HRP) or 0.1 mM H_2DCF with 200 mM glucose (for GOx) was pipetted on top of the gel with immobilized enzyme. The reaction was followed at 528 nm (λ_{ex} = 485 nm).

Stability of the enzyme-gel coupling

Different concentrations of enzymes GOx (0.1, 0.2 and 0.4 nM), HRP (100, 200 and 400 nM) and enzyme mixtures (0.2 nM GOx + 200 nM HRP and 0.4 nM GOx + 400 nM HRP) were immobilized in 100 µL dissolved alginate in 96-well plates. Each well was incubated with 100 µL of PBS pH 6.2 at RT and static conditions, and then the buffer was transferred to a test tube. The incubation was repeated six times with fresh portions of buffer and the incubation times were: 30, 30, 60, 90 min, 24 h and again 24 h. Enzyme activity was analyzed for an eluate volumes of 15 µL of each collected sample at RT using H_2DCF as a second HRP substrate (λ_{ex} = 485 nm and λ_{em} = 528 nm).

Stability and storage of functionalized matrices

0.1 nM GOx and 0.1 nM GOx + 20 nM HRP were immobilized in 100 µL alginate in 96-well plates. The plates were stored at 4 or 30°C and with or without a seal protecting from evaporation. After 0, 1, 5, 9, 19 and 30 days, 100 µL of substrate mix (final 0.1 mM of H_2DCF and 0.1 mM of H_2O_2 for HRP assay and final 200 mM of glucose for GOx assay) was added on top of the gel to initiate the reaction. The increase of the amount of product (DCF) was measured at RT by exciting the sample at 485 nm and detection at 528 nm.

Results and discussion

The multi-parameter wound dressing was developed for two parameters, the biomarker glucose and pH. The sensor's chemical and biological components were characterized before and after the assembly into a sensing matrix.

pH monitoring

The pH has been identified as an ideal parameter to follow the healing process of a wound over time (Milne and Connolly 2014). Since the pH fluctuates in the window between 6 < pH < 8, the rather large pH-changes can be sensitively detected by pH-dependent fluorophores. The fluorescence intensity of dyes mainly depends on the protonation state and hence on the concentration of protons. Thus, the fluorescence of dyes responds sensitively to changes in the pH-value of the environment whenever the pK_a-value of the dye and the environmental pH-value do not differ much. Therefore, the fluorescent pH-sensing dye, 5(6)-carboxynaphthofluorescein (CNF), that has a pK_a-value within the pH-detection window (pK_a 7.6), which makes CNF very sensitive in the desired pH range, was selected. Additionally, CNF possesses a free carboxyl group that can be used for covalent coupling to the sensing matrix. For the coupling procedure, conventional DCC coupling was applied to connect the dye with sugar-based agarose through an ester linkage. The coupled dye was analyzed spectroscopically to determine the change in fluorescence intensity as a function of pH. In order to evaluate the sensitivity of the sensor for the final application, the coupled dye was measured in artificial wound exudate to mimic the wound environment. Fluorescence spectra confirmed that the coupled dye shows a strong change of the fluorescence intensity in the artificial wound exudate (Figure 2 left). For correlation of the change in the fluorescence intensity with changing pH, the emission intensity at λ = 668 nm was selected (Figure 2 right). With a change of the fluorescence intensity of a factor of ~40 between pH 6.0 and 7.7, the dye showed a very strong fluorescence dependency on the pH in the desired pH range.

Coupled enzyme assay and kinetics

The determination of glucose concentration using coupled enzymes is generally simple and fast. However, to obtain accurate results, the activity and ratio of enzymes should be optimized with regard to the assay conditions. The activity of HRP is usually measured with ABTS as substrate, which can be easily followed by absorbance spectroscopy. In order to obtain a fluorescence signal, a fluorescent substrate needed to be converted. We used activated fluorescein (H_2DCF) as alternative substrate in buffer as well as in complex medium. The reaction rate of free HRP was 670 times lower for H_2DCF than for ABTS as substrate (Table S1). Since it was also much lower than the rate of glucose conversion by

GOx, the amount of HRP per one GOx was increased to compensate its lower catalytic efficiency. The optimal ratio of free GOx:HRP was calculated from the k_{cat} values (Table 2) to be 1:100. For immobilization, a 200-fold excess of HRP vs. GOx was used to ensure that HRP was not rate determining in the coupled assay.

To determine saturated substrate concentrations for HRP, first kinetic measurements were performed in PBS and in artificial wound extract (AWE) and are presented on Fig. 3A as full and empty triangular signs. The H_2DCF concentration of 0.1 mM was found to be sufficient to saturate HRP as the reaction rate at this concentration was close to maximal (Fig. 3A, right side), and was kept constant in following assays aiming in the characterization of GOx parameters in solution as well as in alginate gel.

Influence of immobilization on kinetics

The effects of immobilization of the enzymes in alginate were analyzed in PBS and AWE and are presented on the Fig. 3A.

In general, immobilization resulted in a decrease of reaction rate of both enzymes in AWE. The biggest impact of artificial wound extract on the rate was observed for GOx. In comparison to HRP, the immobilized GOx performed much better than the free enzyme in PBS and AWE accordingly. This might be due to a stabilizing effect of immobilization on GOx activity what has been described before for different carriers (Arica and Hasirci 1993; Kozhukharova et al. 1988).

On the other side, immobilization of HRP had a negative influence on the reaction rate. This enzyme requires two substrates for redox reaction, so both H_2DCF and GOx-produced H_2O_2 must diffuse to the active site of HRP and this process may take longer in the gel matrix. Also the different positioning of the enzyme's active center after immobilization can play a major role. The activity of HRP was in general lower towards H_2O_2 and fluorescein in AWE as compared with PBS. AWE has a very complex composition, which includes a variety of oxidative and degradative enzymes (Eming et al. 2010) that may interfere with measurement by interaction with substrates. Nevertheless, the kinetic analyses showed that the enzymes are active in differently complex media and that the fluorescent substrate, H_2DCF, can be oxidized under these conditions through the sensing enzyme cascade (Table 1).

Influence of additives on GOx activity

Enzyme kinetics assays were conducted in presence of the chemicals necessary for the enzyme coupling and gel formation process ($CaCl_2$ and $NaBH_4$) or other compounds abundant in the wound (L-lactate). None of the tested additives had a significant impact on enzyme activity (Fig. 3B). The chosen gel matrix is therefore adequate for immobilization of the sensing molecule of GOx.

Stability of the immobilized enzymes in the polymeric matrix

In order to assess the possible enzyme leakage from the alginate matrix and to control for the efficiency of coupling, an enzyme-release experiment was performed. For this purpose, gels with immobilized GOx (0.1, 0.2 and 0.4 nM), HRP (100, 200 and 400 nM) and enzyme mixture (0.2 nM GOx + 200 nM HRP and 0.4 nM GOx + 400 nM HRP) were incubated for up to two days, while the buffer was exchanged six times (see materials and methods). The portions were collected, assayed for enzyme activity and the outcome was compared with the activity of non-immobilized enzymes stored under the same conditions. Table 2 presents the cumulative activities from PBS portions, which are expressed as percentage of enzyme released from the gel. Around 10% of GOx and HRP were released after 48 h. At the highest HRP concentration (400 nM) 25% were released. Although the enzyme-alginate coupling is covalent, some enzymes molecules may stay unbound in the gel matrix (e.g. in case of enzyme excess) or adsorbed on its surface. The frequent washing with PBS also might have promoted the enzyme release by shifting the equilibrium in the buffer-gel system and removing Ca^{2+} ions needed for gelation (Lee and Mooney 2012). However, for the proposed application (wound healing), fluid exchange would occur less often and the mentioned equilibrium shift would not be so pronounced. Therefore, a lower loss of enzyme would be expected at the proposed maximal HRP concentration of 20 nM.

For potential medical applications, enzymes should stay active for defined periods of time. Immobilization often improves the enzyme activity over time by providing greater resistance to changing conditions and operational stability. Such an effect was observed by us after immobilization of glucose and maltose sensors (Faccio et al. 2016). For application in a wound pad, enzymes should be active for at least the first two stages of the healing process when most of the exudate is produced – depending on the wound type up to two weeks (Velnar et al. 2009). To check the enzyme system stability, 0.1 nM GOx and 0.1 nM GOx + 20

nM HRP were immobilized in microtiter plates. The plates were then stored in four different conditions: at 4 or 30°C and with or without a sealing protecting from evaporation. Enzymes were assayed after 0, 1, 5, 9, 19 and 30 days at room temperature with fluorescein as a second substrate for HRP. Both enzymes were stable at 4 and 30°C when kept in wet conditions, but they lost their activity as soon as the gel matrix dried (sooner at 30°C; Fig. 4A-D). This implicates the use of moist wound pads, like hydrogels, as a carrier for biosensor molecules. It can also be stored at room temperature without loss of activity for at least 1 month.

End-point detection of metabolites

In order to quantify the concentration of metabolite, the measured signal should reflect the metabolite concentration and, in an ideal case, provide a linear response. To test for the linear range of sensor response, immobilized 0.1 nM GOx and 20 nM HRP were incubated with different glucose concentrations (0; 0.1; 0.5; 1; 2.5; 5; 10 and 20 mM) in AWE and the final fluorescence was measured after 6 h. After this time, the recorded signal was linear for concentrations up to 2.5 mM glucose and at higher concentrations it leveled off (Fig. 4E). This might be due to self-quenching (Nichols et al. 2012) of oxidized fluorescein after the long incubation time. Further research will focus on improvement of the signal stability and linearity. Nevertheless, the quantification of glucose in wound liquid is feasible, since the concentration of glucose in the liquid is much lower than in the blood serum and it was shown to be 1.2 mM for chronic wounds and 2 mM for healing wounds (Trengove et al. 1996) in case of humans. Similar concentrations between 0.65 and 2.56 mM were found in wounds of rats (Kossi and Laato 2000).

Conclusions

In this work, a novel, optical biosensor for monitoring of wound healing processes composed of two systems is reported. We are able to monitor two of the most important wound parameters directly related to the differentiation between chronic and healing wounds: pH and glucose concentration. For pH sensing, 5(6)-carboxynaphthofluorescein was integrated into the agarose hydrogel matrix and showed a high sensitivity for changing pH conditions in the pH range of healing wound. This sensor is also very attractive due to its signal reversibility in the conditions of changing wound pH. The coupled-enzyme system

immobilized on alginate detects low glucose concentrations in very complex solutions, like artificial wound exudate. The application of this system can be expanded for other wound metabolites as lactate and uric acid by simply replacing the first enzyme by another oxidase that produces H_2O_2 as side product. The moist hydrogel wound pad with integrated spots for glucose detection could be stored at room temperature for at least one month without affecting the activity.

Our developed system not only provides an exact fluorescence quantification of pH and glucose concentration, but it was also developed to provide colorimetric signal. With that concept, a potential dual-use of the functional pad is envisaged: a) users/patients would have direct, qualitative information on the status of the wound by simply looking at the two sensors; b) when required, doctors could make an exact determination of pH/glucose levels with a fluorescence spectrometer or a portable fluorescence camera. Moreover, the system is cheap, modular and can easily be integrated into existing commercial wound pads with minimal changes on costs making the concept realistic also from an economic point of view. All these features contribute to a potential high versatility of this system and an impact on future wound management.

Acknowledgments

This work was supported by a grant from the Swiss Confederation and funded by Nano-Tera.ch within the Nano-Tera project “Fabrication of fluorescence biosensors in a textile dressing for non-invasive lifetime imaging-based wound monitoring’, FLUSITEX (RTD 2013) that was scientifically evaluated by SNSF. Dagmara Jankowska and Markus Bannwarth equally contributed to this work.

References

Arica, M.Y., Hasirci, V., 1993. J Chem Technol Biot 58(3), 287-292.

Campbell, K.E., Keast, D., Woodbury, G., Houghton, P., 2003. Wounds 15(2), 40-48.

Dargaville, T.R., Farrugia, B.L., Broadbent, J.A., Pace, S., Upton, Z., Voelcker, N.H., 2013. Biosens Bioelectron 41, 30-42.

Ebrahimi, M.M.S., Schonherr, H., 2014. Langmuir 30(26), 7842-7850.

Eming, S.A., Koch, M., Krieger, A., Brachvogel, B., Kreft, S., Bruckner-Tuderman, L., Krieg, T., Shannon, J.D., Fox, J.W., 2010. J Proteome Res 9(9), 4758-4766.

Faccio, G., Bannwarth, M.B., Schulenburg, C., Steffen, V., Jankowska, D., Pohl, M., Rossi, R.M., Maniura-Weber, K., Boesel, L.F., Richter, M., 2016. Analyst 141, 3982-3984.

Grey, J.E., Enoch, S., Harding, K.G., 2006. Brit Med J 332(7536), 285-288.

Hajnsek, M., Schiffer, D., Harrich, D., Koller, D., Verient, V., van der Palen, J., Heinzle, A., Binder, B., Sigl, E., Sinner, F., Guebitz, G.M., 2015. Sensor Actuat B-Chem 209, 265-274.

Kossi, J., Laato, M., 2000. Pathobiology 68(1), 29-35.

Kozhukharova, A., Kirova, N., Popova, Y., Batsalova, K., Kunchev, K., 1988. Biotechnol Bioeng 32(2), 245-248.

Krismastuti, F.S.H., Brooks, W.L.A., Sweetman, M.J., Sumerlin, B.S., Voelcker, N.H., 2014. J Mater Chem B 2(25), 3972-3983.

Lee, K.Y., Mooney, D.J., 2012. Prog Polym Sci 37(1), 106-126.

McColl, D., Cartlidge, B., Connolly, P., 2007. International journal of surgery 5(5), 316-322.

Mehmood, N., Hariz, A., Fitridge, R., Voelcker, N.H., 2014. Journal of biomedical materials research. Part B, Applied biomaterials 102(4), 885-895.

Mehmood, N., Hariz, A., Templeton, S., Voelcker, N.H., 2015. Biomed Eng Online 14.

Milne, S.D., Connolly, P., 2014. J Wound Care 23(2), 53-57.

Milne, S.D., Seoudi, I., Hamad, H.A.I., Talal, T.K., Anoop, A.A., Allahverdi, N., Zakaria, Z., Menzies, R., Connolly, P., 2015. Int Wound J.

Nichols, J.J., King-Smith, P.E., Hinel, E.A., Thangavelu, M., Nichols, K.K., 2012. Invest Ophth Vis Sci 53(9), 5426-5432.

Phair, J., Newton, L., McCormac, C., Cardosi, M.F., Leslie, R., Davis, J., 2011. Analyst 136(22), 4692-4695.

Schneider, L.A., Korber, A., Grabbe, S., Dissemond, J., 2007. Arch Dermatol Res 298(9), 413-420.

Schulenburg, C., Faccio, G., Jankowska, D., Maniura-Weber, K., Richter, M., 2016. Analyst 141(5), 1645-1648.

Sen, C.K., Gordillo, G.M., Roy, S., Kirsner, R., Lambert, L., Hunt, T.K., Gottrup, F., Gurtner, G.C., Longaker, M.T., 2009. Wound Repair Regen 17(6), 763-771.

Thet, N.T., Alves, D.R., Bean, J.E., Booth, S., Nzakizwanayo, J., Young, A.E., Jones, B.V., Jenkins, A.T., 2016. ACS Appl Mater Interfaces 8(24), 14909-14919.

Trengove, N.J., Langton, S.R., Stacey, M.C., 1996. Wound Repair Regen 4(2), 234-239.

Velnar, T., Bailey, T., Smrkoli, V., 2009. J Int Med Res 37(5), 1528-1542.

Widmer, S., Dorrestijn, M., Camerlo, A., Urek, S.K., Lobnik, A., Housecroft, C.E., Constable, E.C., Scherer, L.J., 2014. Analyst 139(17), 4335-4342.

Widmer, S., Reber, M.J., Muller, P., Housecroft, C.E., Constable, E.C., Rossi, R.M., Bruhwiler, D., Scherer, L.J., Boesel, L.F., 2015. Analyst 140(15), 5324-5334.

Figure legends

Figure 1 Scheme of the sensing principle for non-invasive wound monitoring based on the detection of pH-values and glucose concentrations.

Figure 2 Sensing of the pH value in AWE based on a pH-sensitive fluorescent dye. The pH-dependency is especially pronounced in the region of pH = 6-8, which is the most relevant range during the wound healing process (A). The graph (B) shows the increase in the fluorescence intensity with increasing pH at an emission wavelength of 668 nm.

Figure 3 (A) Comparison of enzyme reaction rates in buffer and complex media (PBS buffer or artificial wound extract, AWE). Reaction rates of 0.1 nM GOx and 0.1 nM GOx + 20 nM HRP were measured for enzymes in a free form and after immobilization on alginate. (B) Influence of additive on glucose oxidase activity in the artificial wound extract. The enzyme activity was assayed at 100 mM glucose concentration using ABTS as a second substrate.

Figure 4 (A-D) Storage ability of functionalized matrix at 4°C and 30°C under wet or dry conditions. Reaction rate of immobilized (A) 20 nM HRP stored at 4°C; (B) 20 nM HRP stored at 30°C; (C) 0.1 nM GOx + 20 nM HRP stored at 4°C; (D) 0.1 nM GOx + 20 nM HRP stored at 30°C. (E) The fluorescence of fully converted glucose at different concentrations in PBS (▲) and AWE (◌). Inset: linear range of fluorescent signal for glucose quantification in AWE. (F) Image showing the functionalized wound pad for analysis of the glucose concentrations. Glucose concentrations form left to right: 0; 0.02; 0.5; 2; 5 and 10 mM.

Figure 1

Click here to download high resolution image

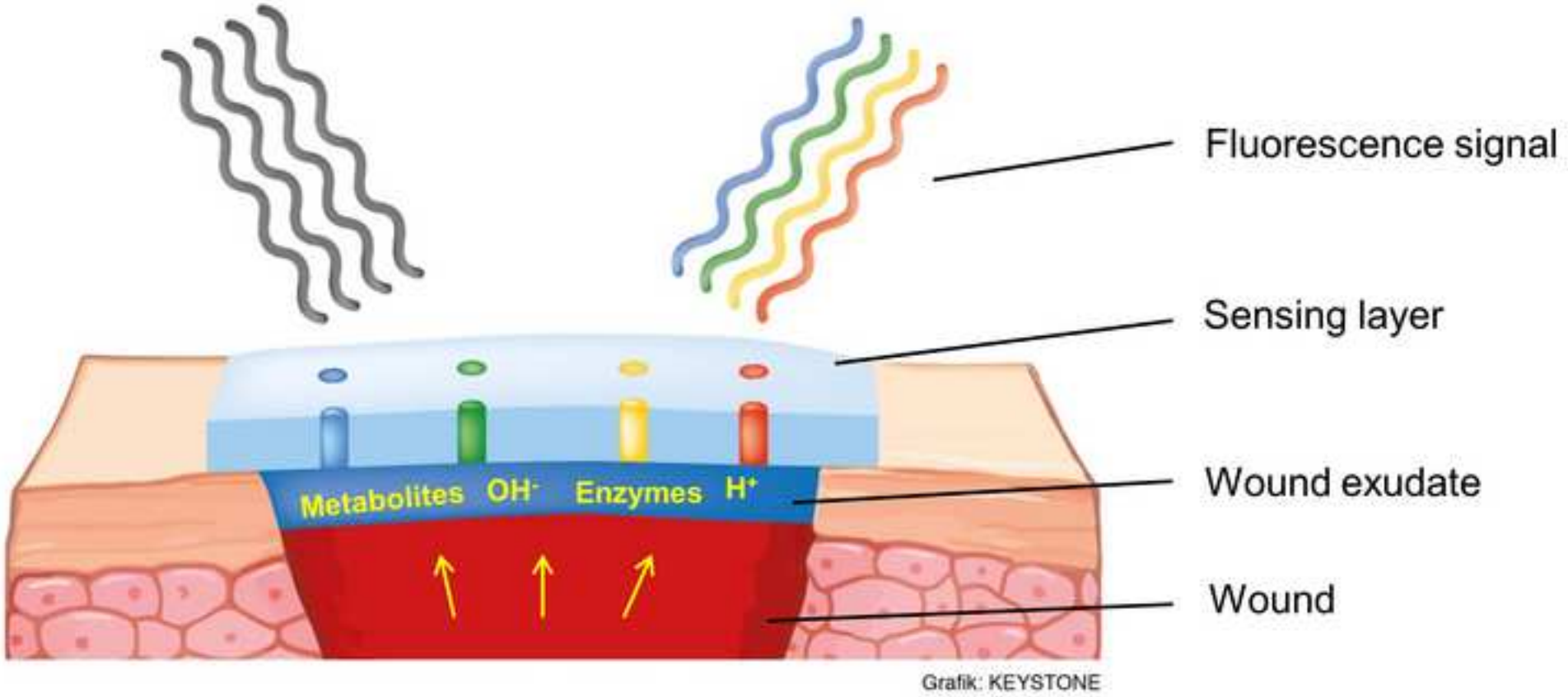

Figure 2

Click here to download high resolution image

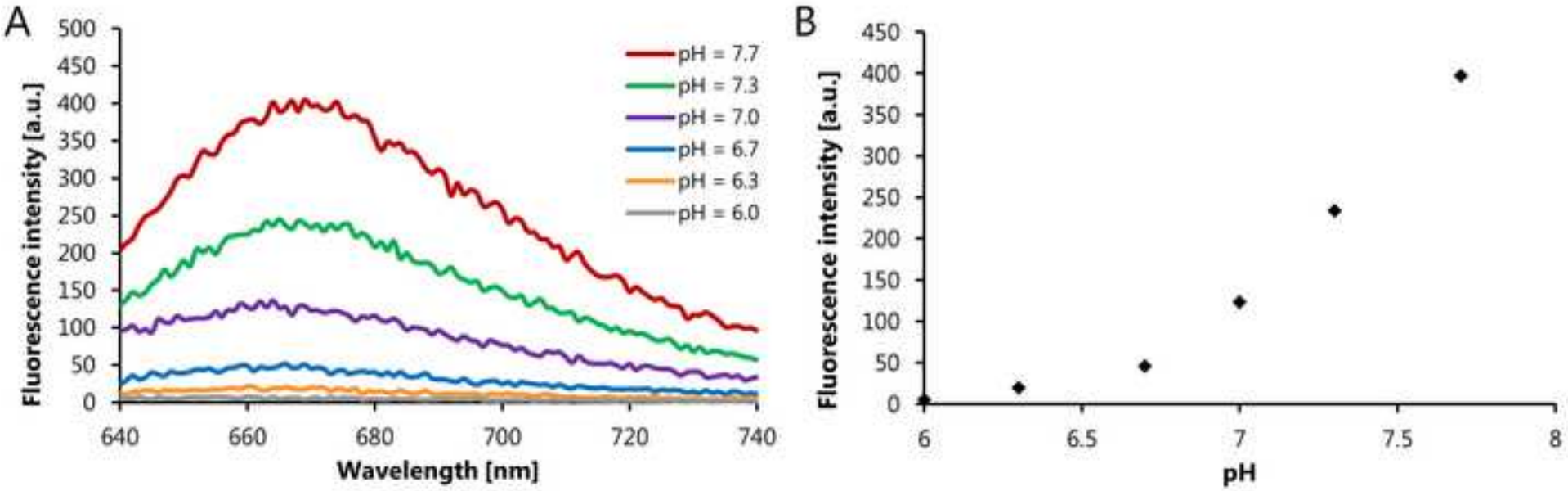

Figure 3

Click here to download high resolution image

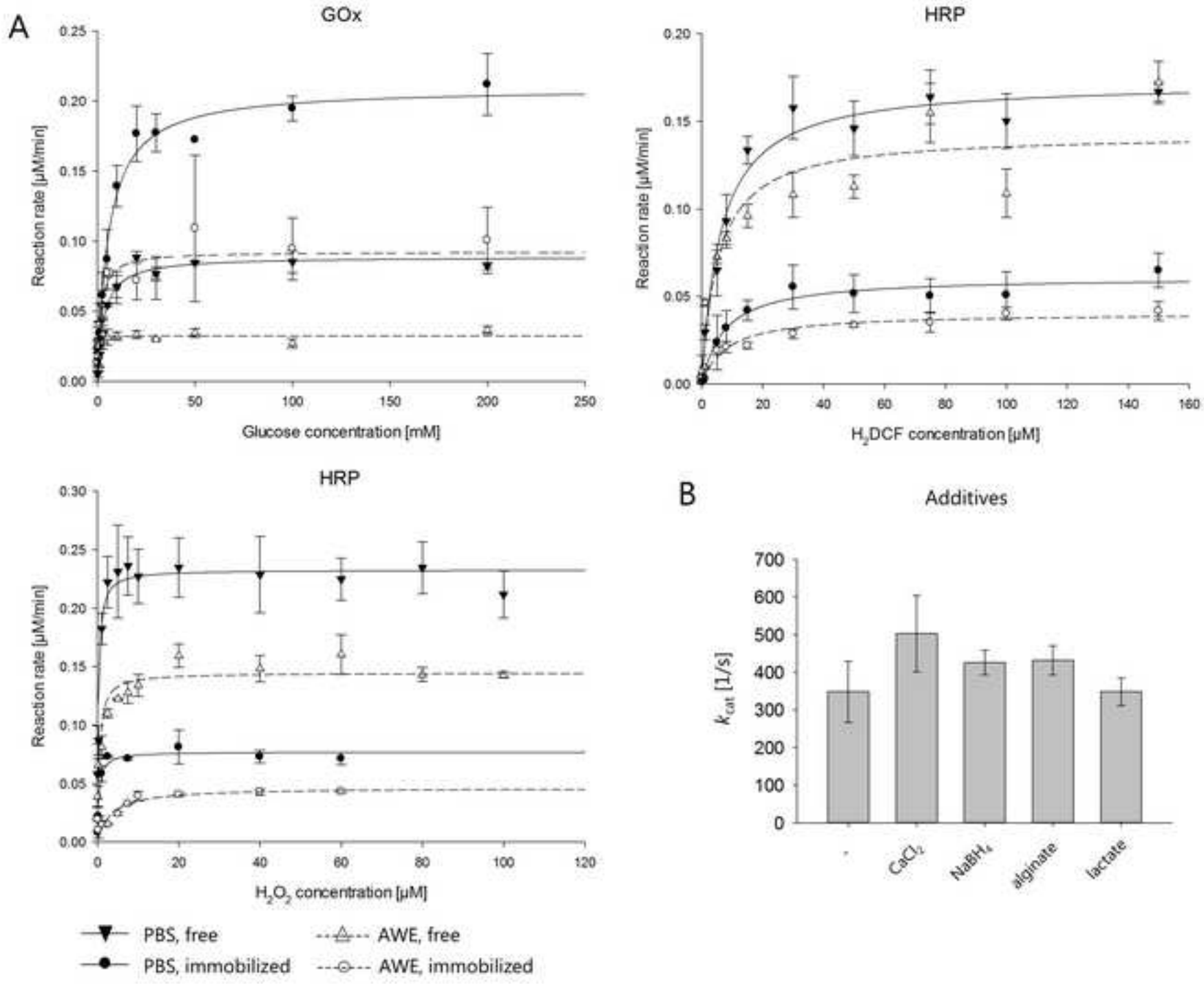

Figure 4

Click here to download high resolution image

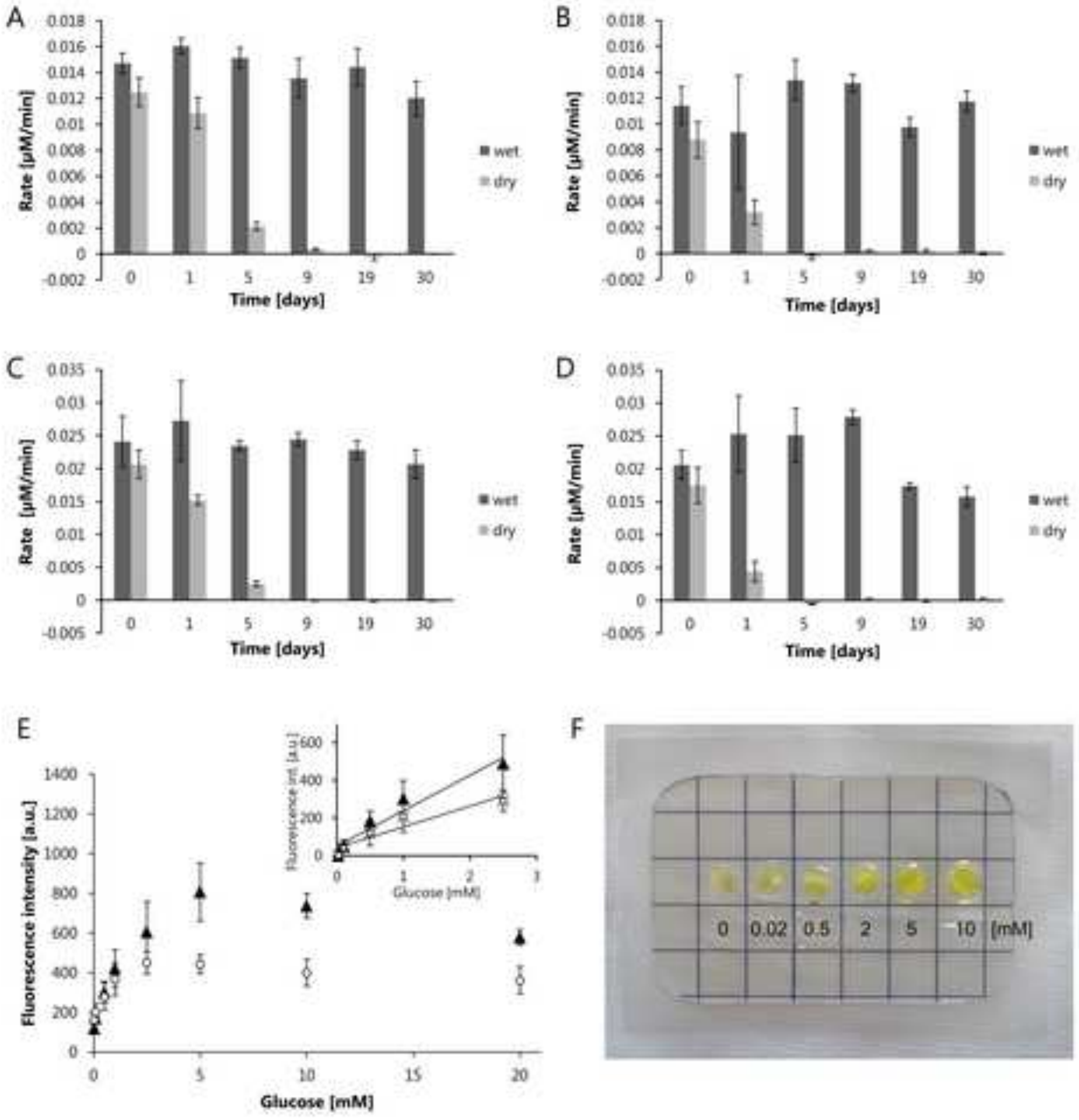

Tables

Table 1 Kinetic parameters of free and immobilized enzymes assayed in PBS and AWE. The experiment was repeated three times with three replicates.

Enzyme assayed	**Enzymes present**	**Condition**	**Substrate**	K_M **[µM]**	k_{cat} **[s^{-1}]**
HRP, immobilized	20 nM HRP	PBS	H_2O_2*	0.37 ± 0.08	0.067 ± 0.002
		AWE	H_2O_2*	3.2 ± 1.8	0.039 ± 0.005
		PBS	H_2DCF**	6.9 ± 1.3	0.045 ± 0.002
		AWE	H_2DCF**	16 ± 4	0.072 ± 0.004
HRP, free	20 nM HRP	PBS	H_2O_2*	0.25 ± 0.05	0.19 ± 0.01
		AWE	H_2O_2*	0.45 ± 0.16	0.12 ± 0.01
		PBS	H_2DCF**	6.2 ± 1.1	0.14 ± 0.01
		AWE	H_2DCF**	2.3 ± 1.4	0.085 ± 0.008
GOx, immobilized	0.1 nM GOx + 20 nM HRP	PBS	glucose	4300 ± 1000	19 ± 2
		AWE	glucose	1000 ± 400	9.1 ±0.7
GOx, free	0.1 nM GOx + 20 nM HRP	PBS	glucose	3200 ± 600	15 ± 1
		AWE	glucose	96 ± 32	5.4 ± 0.2

* Concentration of H_2O_2 varied, whereas concentration of H_2DCF was constant (100 µM)

** Concentration of H_2DCF varied, whereas concentration of H_2O_2 was constant (50 µM)

Table 2 The release of immobilized enzymes from alginate gel after six washing cycles over 48 h.

Enzyme assayed	Immobilized enzymes	Relative activity [%]
GOx	0.1 nM GOx	12 ± 2
	0.2 nM GOx	9 ± 2
	0.4 nM GOx	8 ± 2
	0.2 nM GOx + 200 nM HRP	5 ± 1
	0.4 nM GOx + 400 nM HRP	7 ± 1
HRP	100 nM HRP	12 ± 3
	200 nM HRP	13 ± 3
	400 nM HRP	25 ± 6
	0.2 nM GOx + 200 nM HRP	2 ± 1
	0.4 nM GOx + 400 nM HRP	7 ± 3